Structure and specificity of lamprey monoclonal antibodies

Brantley R. Herrin*†‡§, Matthew N. Alder*†‡§, Kenneth H. Roux¶, Christina Sina∥, Götz R. A. Ehrhardt*†‡§, Jeremy A. Boydston‡, Charles L. Turnbough, Jr.‡, and Max D. Cooper*†‡§**

Departments of *Medicine, †Pediatrics, ‡Microbiology, and §Pathology, University of Alabama at Birmingham, Birmingham, AL 35294; ¶Department of Biological Science, Florida State University, Tallahassee, FL 32306; and ∥University of Kiel, 24098 Kiel, Germany

Adaptive immunity in jawless vertebrates (lamprey and hagfish) is mediated by lymphocytes that undergo combinatorial assembly of leucine-rich repeat (LRR) gene segments to create a diverse repertoire of variable lymphocyte receptor (*VLR*) genes. Immunization with particulate antigens induces VLR-B-bearing lymphocytes to secrete antigen-specific VLR-B antibodies. Here, we describe the production of recombinant VLR-B antibodies specific for BclA, a major coat protein of *Bacillus anthracis* spores. The recombinant VLR-B antibodies possess 8–10 uniform subunits that collectively bind antigen with high avidity. Sequence analysis, mutagenesis, and modeling studies show that antigen binding involves residues in the β-sheets lining the VLR-B concave surface. EM visualization reveals tetrameric and pentameric molecules having a central core and highly flexible pairs of stalk-region "arms" with antigen-binding "hands." Remarkable antigen-binding specificity, avidity, and stability predict that these unusual LRR-based monoclonal antibodies will find many biomedical uses.

antigen-binding site | leucine-rich repeat | variable lymphocyte receptor

The adaptive immune system in jawless vertebrates (agnathans) is comprised of clonally diverse lymphocytes that express variable lymphocyte receptors (VLRs) created by the combinatorial assembly of leucine-rich repeat (LRR) gene segments rather than the Ig V, D, and J gene segments used by jawed vertebrates (gnathostomes) (1, 2). Two *VLR* genes, *VLR-A* and *VLR-B*, have been identified in both lamprey and hagfish (1–3). The germline VLR genes are incomplete in that they have coding regions only for the invariant N-terminal and C-terminal sequences, which are separated by intervening sequences, lacking canonical splice sites (1, 2). During development of lymphocyte lineage cells, components of the flanking LRR modular units are sequentially inserted into the incomplete VLR gene with a concomitant deletion of the intervening sequences (4, 5). The stepwise assembly of a mature VLR gene is mediated via a gene conversion mechanism in which AID-APOBEC family members with lymphocyte-restricted expression may serve a catalytic role (3, 5). This somatic gene rearrangement process has been estimated to produce a potential repertoire of $>10^{14}$ distinct VLR-B receptors (4).

VLR-B proteins constitute a major component of the humoral arm of the lamprey adaptive immune system. Earlier studies, before the discovery of *VLR* genes, established that lampreys produce serum antibody-like proteins with agglutination and neutralization activity in response to immunization with particulate antigens, such as bacteriophage, *Brucella abortus*, and human red blood cells (6–10). More recently, we demonstrated that immunization with *Bacillus anthracis* exosporium induces production of soluble, antigen-specific VLR-B proteins, much like the antibody responses of jawed vertebrates (4). The secreted VLR-B proteins may function analogously to antibodies in jawed vertebrates, whereby microbe-induced VLR-B antibodies promote clearance of the infectious agent, presumably by neutralization, opsonization, and other mechanisms.

Monoclonal antibodies are valuable research and therapeutic tools that take advantage of the remarkable ability of the jawed vertebrate adaptive immune system to recognize almost any foreign molecule. In theory, it should also be possible to capitalize on the tremendous repertoire diversity of the agnathan adaptive immune system to produce cloned VLR-B antibodies of known specificity, with similar properties to monoclonal antibodies. However, there is no long-term *in vitro* culture system for lamprey lymphocytes, nor are there means to immortalize them presently, and the lack of fusion partner cell lines precludes the use of hybridoma fusion technology. Here, we describe a method of producing soluble, recombinant monoclonal VLR-B antibodies of defined antigen specificity and use them to investigate the quaternary structure and antigen binding site of secreted VLR-B antibodies.

Results

Production of Recombinant, Antigen-Specific VLR-B Antibody Clones. To generate VLR-B antibody-producing cells, we developed a heterologous expression system in which HEK-293T cells were transfected with full-length VLR-B cDNAs derived from lymphocytes of lamprey larvae immunized with the exosporium (i.e., the outermost layer) of *B. anthracis* spores [supporting information (SI) Fig. 5]. Clones that secreted antigen-specific VLR-B antibodies into the culture supernatant were then identified by ELISA and immunofluorescence-based flow cytometry assays. The secreted recombinant VLR-B antibodies are large molecules similar in molecular weight to primary VLR-B antibodies in plasma samples (SI Fig. 6). Fourteen of 212 VLR-B transfectants (6.6%) were found to secrete VLR-B antibodies against the C-terminal domain of the major exosporium protein BclA (BclA-CTD) (11, 12), a major epitope recognized by primary VLR-B antibodies made in the lamprey response. We selected the eight recombinant antibodies that recognized BclA-CTD at the highest levels above background and one weakly binding clone, VLR5, for more comprehensive analysis (Fig. 1*A*). Seven of the eight BclA-CTD-reactive clones were also reactive with wild-type *B. anthracis* spores, but not BclA-deficient *B. anthracis* spores (ΔBclA) or strains of two closely related *Bacillus* species, *Bacillus cereus* T and *Bacillus thuringiensis* (subsp. Kurstaki) in ELISA (Fig. 1*B*) and flow cytometry (Fig. 1*C*) assays. *B. anthracis* BclA-CTD differs from *B. cereus* T BclA-CTD at 14 of 134 amino acid positions, only 9 of which are solvent exposed (SI Fig. 7) (13). These results indicate that monoclonal VLR-B antibodies can discriminate between closely related protein antigens on the basis of limited amino acid variation.

Fig. 1. Production of monoclonal VLR-B antibodies specific for BclA-CTD of *B. anthracis*. (*A*) VLR-B antibody clones expressed by HEK-293T cells detect recombinant BclA-CTD by ELISA. NT indicates supernatant from nontransfected cells. (*B* and *C*) VLR-B antibody clones specifically detect *B. anthracis* spores by ELISA (*B*) and flow cytometry (*C*). ΔBclA, BclA-deficient *B. anthracis* spores.

The recombinant VLR-B antibodies that reacted strongly with both recombinant BclA-CTD and *B. anthracis* spores were all different by sequence analysis (SI Fig. 8). However, most shared the same number of LRR units and displayed notable sequence similarity, even in hypervariable amino acid positions. To evaluate how the shared residues might contribute to BclA-CTD binding, we constructed a homology-based model of the VLR4 structure by using the crystal structure of hagfish VLR-B (14) as a template (Fig. 2). The amino acids in hypervariable positions of neighboring LRR units were located near each other in the potential antigen binding site on the concave surface of the VLR-B antibody. A deep pocket contributed by residues of the LRRV, LRRVe, and LRR-CP units in the center of the concave surface may form a complementary surface for BclA-CTD binding. The LRR-CT sequences of the BclA-CTD-specific clones were identical except for a small variable region consisting of two to three residues (Fig. 2B). Our model predicts that the variable residues are located at the tip of the loop formed by the LRR-CT that projects toward the concave surface. This suggests that the variable amino acids of the LRR-CT may contribute to antigen binding.

Secreted VLR-B Antibodies Are Composed of Disulfide-Linked Pentamers and Tetramers of Dimers. The BclA-CTD-specific recombinant VLR4 antibody was purified by antigen affinity chromatography to examine its quaternary structure. Although this antibody could not be eluted from a BclA-CTD affinity column by high salt concentrations or extreme acidic conditions (pH < 1.5), it could be dissociated by very basic conditions (pH > 11) (SI Fig. 9A). Despite these harsh conditions, the eluted VLR4 antibody retained full antigen binding ability even after storage for >12 months at 4°C, 1 month at room temperature, or 36 h at 56°C (data not shown). Two forms of the recombinant VLR4 antibody, both larger than 225-

Fig. 2. A model of the putative antigen binding surface of a BclA-CTD-specific VLR-B antibody. (*A*) Homology-based model of the tertiary structure of clone VLR4 constructed by using the crystal structure coordinates of hagfish VLR-B (PDB ID codes 2O6R and 2O6S) as a template. (*Upper*) Frontal view. (*Lower*) Side view. Hypervariable positions of each LRR module are indicated by color: LRR-NT (blue), LRR1 (light blue), LRRV (green), LRRVe (light green), CP (yellow), and LRR-CT (orange). (*B*) Alignment of the LRR-CT sequences of VLR-B clones specific for BclA-CTD. Invariant residues are shaded black, and variable residues are shaded orange.

kDa molecular mass standards, were eluted from the BclA-CTD affinity column (SI Fig. 9B). To obtain an accurate estimate of the molecular mass of VLR4, Ferguson plots were constructed by comparing the relative mobility of VLR4 and molecular mass standards in native gels of 5–12% acrylamide. The data indicated a molecular mass of 400 kDa for the larger VLR4 band (Fig. 3A), whereas a molecular mass of 40 kDa was estimated for individual VLR4 monomeric units. Therefore, the largest VLR4 oligomer may have 10 subunits, and the lower molecular mass VLR4 oligomer may contain 8 VLR subunits. Notably, a partially reduced band of 80 kDa, indicative of dimeric subunits, was observed on Western blots after exposure to relatively low concentrations of reducing agents (Fig. 3B). To visualize this structure, purified VLR4 antibody was examined by negative stain transmission electron microscopy (TEM). Pentameric VLR4 molecules with thin, highly flexible arms were observed, wherein the basally connected dimeric subunits form a central consolidation (Fig. 3C). Structurally similar VLR4 tetramers were also seen (data not shown). The composite results suggest that oligomeric VLR-B antibodies are composed of
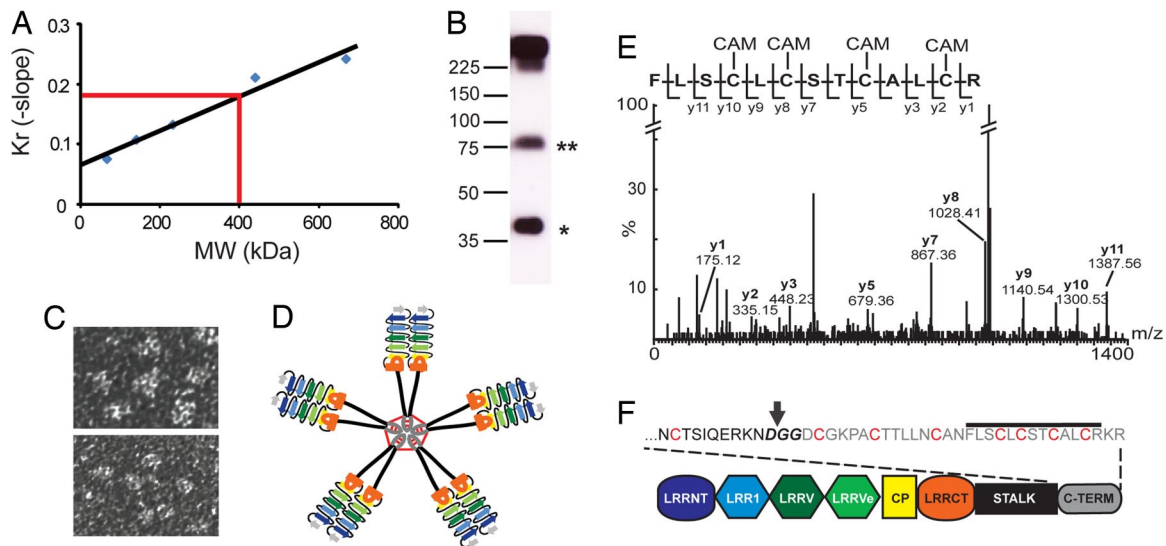
IMMUNOLOGY

Fig. 3. Quaternary structure of secreted VLR-B antibodies. (*A*) Molecular mass estimate of a purified recombinant VLR-B antibody (VLR4) by Ferguson plot analysis. Blue dots, Molecular mass standards; red line, VLR4. (*B*) Western blot of a partially reduced VLR-B antibody; monomeric (*) and dimeric (**) subunits of the partially reduced antibody. (*C*) Negative stain TEM of VLR4. (*Upper*) Pentameric arrangement of VLR-B subunits. (*Lower*) Flexibility of subunits. (*D*) A model of VLR-B antibody quaternary structure with red lines representing disulfide bonds. (*E*) MS/MS sequencing of tryptic fragments of reduced VLR4. Ions matching the sequence of the C terminus of VLR4 are labeled in the spectrograph. CAM indicates carboxyamidomethylation of cysteine by iodoacetamide. (*F*) Cartoon depicting the location of the cysteine-rich peptide in the VLR-B antibody. The predicted GPI cleave site (bold text) is indicated by an arrow, cysteines that may form intermolecular disulfide bonds are highlighted red, and the peptide detected in *E* is indicated by a line above the text.

four or five disulfide-linked dimeric subunits, somewhat like IgM antibodies (Fig. 3*D*).

The multivalent structure of VLR4 suggested that it could function as a potent agglutinin. To examine this potential, we compared the ability of the VLR4 antibody versus an anti-BclA-CTD mouse monoclonal antibody (EA2-1; IgG2b) (15) to agglutinate wild-type *B. anthracis* spores (SI Fig. 10). Equal concentrations of VLR4 and EA2-1, starting at 0.5 mg/ml, were serially diluted in 10-fold increments and scored for the degree of spore agglutination. Spore agglutination by VLR4 was detected at a concentration 1,000-fold more dilute (5 pg/ml) than the mouse monoclonal antibody (5 ng/ml). This finding indicates that monoclonal VLR-B antibodies can possess high avidity for an antigen with repetitive epitopes because of the multimeric arrangement of the antigen-binding subunits.

The Cysteine-Rich C Terminus Is Required for Assembly of Monomeric VLR-B Peptides into Multivalent Antibodies. The VLR-B antibody multimeric structure raises the question of how these molecules are assembled and released, especially given that cell surface VLR-B molecules are tethered by GPI linkage (1). If VLR-B antibodies were released by cleavage of the GPI linkage, the cysteines used for oligomerization of solubilized VLR-B antibodies would have to be N-terminal to the GPI cleavage site, because amino acids C-terminal to the cleavage site would be removed by GPI addition in the endoplasmic reticulum. To examine this possibility, trypsinized peptides of the purified VLR4 antibody were sequenced by tandem mass spectrometry. This analysis revealed that the entire cysteine-rich peptide sequence of the C terminus is present in the secreted multimeric VLR4 antibody, thus indicating that secreted VLR-B antibodies are not derived from a GPI-linked precursor. These results also suggest that the cysteines responsible for oligomer formation are located in the relatively hydrophobic C terminus of the VLR-B antibody (Fig. 3 *E* and *F*). To test this prediction, we expressed a construct encoding the VLR4 antibody beginning with the start codon and extending to the GPI cleavage site (VLR4$^{GPI-stop}$) in HEK-293T

cells. The truncated VLR4$^{GPI-stop}$ and wild-type VLR4 (VLR4^{WT}) molecules produced by transfectants were separated by nonreducing SDS/PAGE, and their molecular weights were estimated by Western blotting. As predicted, the VLR4$^{GPI-stop}$ molecule migrated as a ≈40-kDa monomer (SI Fig. 11*A*). ELISA evaluation of antigen binding by the oligomeric VLR4^{WT} versus the monomeric VLR4$^{GPI-stop}$ antibodies indicated strong BclA-CTD binding by the oligomeric VLR4 antibody and weak antigen binding by the monomeric VLR4 antibody (SI Fig. 11*B*). These results imply that, even though VLR-B monomeric units have a relatively low antigen binding affinity, the antigen binding avidity of a multimeric VLR-B antibody can be relatively high.

The β-Sheets on the Concave Surface of VLR-B Antibodies Constitute the Primary Antigen Binding Site. Because of their high sequence variability, the parallel β-strands that form the concave surface of VLR-B are presumed to be the antigen binding site (4, 14). However, this assumption has not been experimentally tested. The amino acid sequences of four BclA-CTD-specific VLR-B antibodies are similar in the predicted antigen binding region, and three of these (VLR4, Ba41, and Ba191) bind BclA-CTD with relatively high avidity. The other, VLR5, exhibits weak antigen binding, and its sequence differs from the consensus sequence of the high-avidity BclA-CTD VLR-B antibodies at 6 of 20 possible hypervariable amino acid positions on the concave surface (H34, Y55, T58, Q101, S103, W127) (Fig. 4 *A* and *B*). These findings suggest that one or more of these six residues causes the relatively low antigen avidity of the VLR5 antibody. To test this hypothesis, we used site-directed mutagenesis to change the variant VLR5 residues to the corresponding amino acids in VLR-B antibodies with higher antigen binding avidity. By using surface plasmon resonance to evaluate antigen binding by VLR4^{WT}, VLR5^{WT}, and VLR5 mutants with modifications of the posited antigen binding site (VLR5^{H34N}, VLR5^{Y55R}, VLR5^{T58I}, VLR5^{Q101H}, VLR5^{S103A}, and VLR5^{W127Y}), we observed much higher binding responses to BclA-CTD for VLR5^{Y55R}, VLR5^{T58I}, and VLR5^{W127Y} relative to the VLR5^{WT} antibody. The response curves were indicative of an increase in the
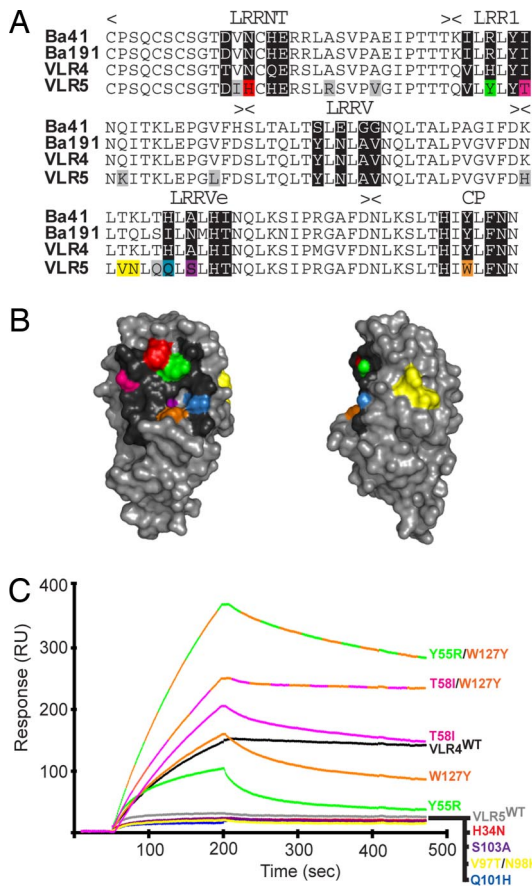
Fig. 4. The primary antigen binding site of VLR-B is located on the concave surface. (*A*) Sequence alignment of high-avidity (Ba41, Ba191, VLR4) and low-avidity (VLR5) VLR-B antibodies specific for BclA-CTD. Hypervariable positions are shaded black. Amino acids in VLR5 that differ from the high-avidity clones are shaded in color if they are in hypervariable positions or gray if located elsewhere, except V97/N98 (yellow). (*B*) Homology-based model of VLR5 structure. Amino acids in hypervariable positions are color-coded as in *A*. (*C*) Surface plasmon resonance measurement of the interaction between VLR4^WT, VLR5^WT, or VLR5 mutant antibodies with BclA-CTD. VLR5 residues in hypervariable positions that differ from the high-avidity clones were mutated to the consensus amino acid of the high-avidity clones at that position. Response curves are color-coded with respect to amino acid positions depicted in *A* and *B*.

association rate of these VLR5 mutants with BclA-CTD; however, the VLR:BclA-CTD complexes formed by these VLR5 mutants dissociated more rapidly than VLR4 (Fig. 3*C*). The other VLR5 mutants (VLR5^H34N, VLR5^Q101H, VLR5^S103A) displayed equivalent or slightly weaker binding avidity when compared with the VLR5^WT antibody (Fig. 4*C*).

Because mutation of the Y55, T58, or W127 residues on the concave surface increased VLR5 antigen binding avidity, we made double mutants of VLR5 (Y55R/W127Y and T58I/W127) to test whether these residues could function in a cooperative manner for antigen binding (Fig. 4*C*). Both the VLR5^Y55R/W127Y and VLR5^T58I/W127Y double mutants exceeded the antigen binding response of their single mutation counterparts and their rate of dissociation was more comparable with that of the VLR4 antibody, indicative of enhanced binding avidity. In contrast, when we mutated two residues of VLR5 that differ from the corresponding residues of the high-avidity clones, but that are not located on the concave surface (V97T/N98K), BclA-CTD antigen binding response of this mutant was similar to that of VLR5^WT. These results suggest that the hypervariable amino acids on the concave surface are the primary antigen binding residues.

Discussion

We have developed a method to exploit the vast repertoire diversity of the lamprey adaptive immune system to produce recombinant monoclonal VLR-B antibodies with high avidity and specificity for antigen. VLR-B antibody clones discriminated *B. anthracis* from *B. cereus* spores with 100% accuracy (seven of seven clones tested), despite 89.5% identity (120 of 134 aa) in peptide sequences of BclA-CTD from *B. anthracis* and *B. cereus*. Monoclonal VLR-B antibodies also agglutinated *B. anthracis* spores at a 1,000-fold higher dilution than an IgG2b monoclonal antibody, demonstrating the high avidity of the multivalent VLR-B antibodies for antigens with repetitive epitopes. The high avidity of VLR-B antibodies facilitated their purification from crude supernatant by antigen affinity chromatography. Surprisingly, VLR-B antibodies could not be eluted by high salt concentrations or extreme acidic conditions (pH <2.0). Although highly basic solutions (pH >11) were required to elute VLR-B antibodies, the structure and antigen binding activity of the antibodies was not compromised by the harsh conditions. Recombinant VLR-B antibodies also retained their antigen binding activity after prolonged exposure to high temperatures, including 1 month at room temperature and 36 h at 56°C. These studies indicate that the LRR subunits form a very stable structure that should be resistant to denaturation under most storage and assay conditions.

Lampreys produce multivalent serum antibodies with high antigen binding avidity even though the constituent VLR units exhibit relatively low affinity for antigen. Recombinant VLR-B antibodies are assembled into disulfide-linked tetramers and pentamers of dimers with approximate molecular weights of 320 and 400 kDa, respectively. The molecular weight estimates are remarkably similar to previous estimates of lamprey agglutinins, although not all of the biochemical properties ascribed to the agglutinins are consistent with VLR-B antibodies (i.e., lack of interchain disulfide bonds) (9). The pentameric/tetrameric arrangement of VLR-B subunits is similar to the subunit organization of IgM antibodies in higher vertebrates. Notably, however, VLR-B antibodies use monomeric subunits for antigen binding rather than the heterodimeric pairing of heavy and light chain peptides that form the antigen binding surface of most jawed vertebrate antibodies. The single peptide composition of VLR-B antibodies makes them more amenable to molecular engineering, including manipulation of the antigen binding site by mutagenesis and fusions to the coding sequences of other peptides, such as enzymes, toxins, and epitope tags to extend their functional capabilities. Furthermore, it may be possible to use random mutagenesis technologies to create libraries of VLR-B antibodies with higher affinity for antigen than can be produced *in vivo* to promote monomeric VLR-B antigen binding.

In conclusion, our studies reveal several unique and potentially advantageous characteristics of monoclonal VLR-B antibodies. Multivalency contributed by 8–10 identical antigen binding subunits assures relatively high-avidity binding to antigens with repetitive epitopes. In contrast with typical IgM antibodies, the VLR-B antibodies that we have examined are relatively stable and appear to have limited cross-reactivity. This difference in specificity may be because VLR-B antibodies use β-sheets as the primary antigen binding surface, whereas Ig-based antibodies use extended loops for antigen binding. The ease of mutational modification of the antigen binding site of VLR-B antibodies should allow their binding characteristics to be tailored to the requirements of a particular assay. Finally, VLR-B antibodies may be produced against mammalian antigen epitopes that would be forbidden for Ig-based antibodies because of self-tolerance.

Methods

Animals and Immunization. Two- to 4-year-old lamprey larvae were maintained and immunized as previously described (4). All experiments were approved by Institutional Animal Care and Use Committee at the University of Alabama at Birmingham.

VLR-B cDNA Library Cloning. Blood samples collected from immunized, lethally anesthetized lamprey were centrifuged at $50 \times g$ for 5 min to pellet red blood cells, and then buffy coat leukocytes overlaying the red blood cell pellet were collected by pipetting. VLR-B$^+$ lymphocytes labeled with anti-VLR-B mAb (4C4) (specific for the invariant stalk region) (4) were purified by using a MoFlo cell sorter (DakoCytomation). RNA isolated from VLR-B$^+$ lymphocytes with TRIzol (Invitrogen) was reverse transcribed into cDNA by using SuperScript III reverse transcriptase (Invitrogen) and random hexamer priming. VLR-B transcripts were amplified from VLR-B$^+$ lymphocyte cDNA by nested PCR using KOD high-fidelity DNA polymerase (Novagen). The first round of PCR used primers from the 5′- and 3′-untranslated region, LRR_N.F1 (CTCCGCTACTCGGCCTGCA) and LRR_C.R2 (CCGCCATCCCCGAC-CTTTG), respectively. PCR conditions were 25 cycles at 95°C, 30 s; 60°C, 30 s; and 70°C, 1.5 min. The second round of PCR used a 5′-phosphorylated primer, pIRES-koz-fwd (CCACCATGTGGATCAAGTGGATCGCC) and a 3′ primer containing a NheI site, pIRES-NheI-rev (GAGAGCTAGCTCAACGTTTCCTGCAGAGGGC). PCR conditions were 30 cycles at 95°C, 30 s; 62°C, 30 s; and 70°C, 1.5 min. PCR products were purified and digested with NheI (New England Biolabs). More than 500 VLR-B sequences from GenBank were examined for restriction enzyme cut sites; NheI sites were not found in any of the sequences. The NheI-digested PCR products were ligated into the EcoRV and NheI sites of pIRES-puro-2 (Clontech) and transformed into NovaBlue competent cells (Novagen). Individual library colonies were picked and purified with the 96-well format QIAprep 96 Turbo miniprep kit (Qiagen) (clones Ba1–Ba192). In a pilot screen, plasmids were purified from 30 colonies by using QIAprep spin miniprep kit (Qiagen) (clones VLR1–VLR30).

Recombinant VLR-B Expression and Purification. For library screening, purified library plasmids were transfected into HEK-293T cells cultured in RPMI medium 1640 containing 5% FBS using linear polyethylenimine (PEI), molecular weight (MW) 25,000 (Polysciences) at a 3:1 PEI-to-DNA ratio. Supernatants harvested 48 h posttransfection were cleared by centrifugation for 15 min at $20,000 \times g$. Recombinant VLR-B production was verified by Western blotting transfectant supernatants with anti-VLR-B mAb (4C4) and HRP-conjugated polyclonal goat anti-mouse IgG Ab (Southern Biotech). For large-scale protein expression, stable cell lines of HEK-293T cell lines were selected with 2 μg/ml puromycin (Cellgro). Stable cell lines were expanded in standard culture flasks, and then transferred to a CELLine AD 1000 (Integra Biosciences) bioreactor flask for high-density cell culture. VLR4-containing supernatants harvested 5–7 days were cleared by centrifugation and stored in 20 mM MOPS and 0.02% sodium azide buffer, pH 7.2. Recombinant VLR4 was purified by antigen affinity chromatography. Briefly, BclA-1-island-6HIS (BclA-CTD containing the first collagen-like repeat) was covalently coupled to NHS-activated Sepharose beads (GE Healthcare Life Sciences) according to manufacturer's instructions. VLR4-containing supernatant was passed over the BclA-1-island column, which was washed with PBS before elution of VLR-B with 0.1 M triethylamine, pH 11.5, into a tube containing 0.5 ml of 1 M Tris, pH 6.8, dialysis into 10 mM Hepes, 150 mM NaCl, 0.02% sodium azide, pH 7.2, and concentration.

VLR-B Library Screening. For ELISA, plates coated with 5 μg/ml recombinant GST control protein or BclA-CTD-GST were blocked with 1% BSA before incubation with VLR-B transfectant supernatant. VLR-B antibodies were detected with anti-VLR-B mAb (4C4) followed by alkaline phosphatase-conjugated goat anti-mouse IgG polyclonal Ab (Southern Biotech). For spore ELISA, 96-well plates coated with 50 μg/ml poly-L-lysine (Sigma-Aldrich) were washed with water before adding 1×10^6 spores per well and air drying overnight. Spore-coated plates were blocked with 1% BSA before incubation with VLR-B transfectant supernatant. For spore detection by flow cytometry, 1×10^6 spores per well were aliquoted into 96-well round-bottom plates and pelleted by centrifugation at $3,000 \times g$. Spores incubated with VLR-B transfectant supernatants and washed with PBS were incubated with anti-VLR-B mAb (4C4) and then with R-phycoerythrin (RPE)-conjugated goat anti-mouse IgG polyclonal Ab (Southern Biotech). For nonstained controls, spores were incubated with mock-transfected HEK-293T cell supernatant, washed, and then incubated with anti-VLR-B mAb (4C4) followed by RPE-conjugated goat anti-mouse IgG polyclonal Ab.

VLR-B Sequence Analysis and Structural Modeling. VLR-B sequence analysis and multiple sequence alignments were prepared by using VectorNTI (Invitrogen) and GeneDoc (http://www.psc.edu/biomed/genedoc). Homology-based models of VLR4 and VLR5 structure were constructed with MODELLER 9v2 (www.salilab.org/modeller) using the crystal structures of hagfish VLR-B as the template [Protein Data Bank (PDB) ID codes 2O6R and 2O6S].

Ferguson Plots. Purified recombinant VLR4 and high MW standards (thyroglobulin, 669 kDa; ferritin, 440 kDa; catalase, 232 kDa; lactate dehydrogenase, 140 kDa; and BSA, 67 kDa) (GE Healthcare) were separated by electrophoresis using native gels containing 5%, 6%, 8%, 10%, and 12% acrylamide. After electrophoresis, proteins were visualized by Gelcode blue staining (Pierce). The relative mobility (R_f) of VLR4 and each of the MW standard proteins in each percent acrylamide gel was measured. A graph of $\log(100R_f)$ versus percent acrylamide was constructed for each protein and the retardation coefficient (K_r) of each protein was calculated from the negative slope of the line. The K_r value of each MW standard protein was plotted versus its MW to construct a standard curve, from which the MW of VLR4 was calculated.

Electron Microscopy. Negative-stain electron microscopy was performed as previously described (16). Briefly, VLR4 was diluted to 1.25 μg/ml BSB (0.1 M H_3BO_3, 0.025 M $Na_2B_4O_7$, 0.075 M NaCl, pH 8.3), affixed to carbon support membrane. The membrane was stained with 1% uranyl formate and mounted on 600 mesh copper grids for analysis. Electron micrographs were recorded at $\times100,000$ magnification at 100 kV on a JEOL JEM 1200 electron microscope.

Mass Spectrometry. For peptide sequencing by tandem mass spectrometry, recombinant VLR4 was separated on a reducing SDS/PAGE gel and stained with Gelcode blue (Pierce). VLR4 was excised from the gel, alkylated with iodoacetamide, and digested with trypsin. The trypsinized peptides were separated by reverse-phase high-performance liquid chromatography and sequenced by electrospray ionization MS/MS.

Agglutination Assay. Stock solutions of the VLR4 antibody and anti-BclA-CTD mouse monoclonal antibody (EA2-1) (IgG2b) (11) at 0.5 mg/ml were prepared in PBS, and then serially diluted in 10-fold increments from 1/10 to 1/10^{10}. EA2-1 was provided by John F. Kearney (University of Alabama at Birmingham). A total of 100 μl of each antibody dilution was added to 1×10^6 *B. anthracis* spores in 96-well flat-bottom plates and incubated at room temperature before visual inspection for spore agglutination by light microscopy. Spore agglutination was scored on an arbitrary scale from 0 to 4 (0, single spores; 1, clusters of 2–3 spores; 2, clusters of 4–6 spores; 3, clusters of 7–10 spores; 4, large clusters of >10 spores).

Surface Plasmon Resonance Measurements of Antigen Binding Site Mutants. VLR5 antigen binding site mutants were constructed by using QuikChange Site-Directed Mutagenesis (Stratagene). Tissue culture supernatants of HEK-293T cells transfected with VLR4, VLR5^{WT}, and VLR5 mutants were collected 48 h after transfection. VLR expression in the supernatants was detected Western blotting with anti-VLR-B mAb (4C4) and quantitated by densitometry. Supernatants were normalized for VLR expression by dilution in culture media based on densitometry measurements. For surface plasmon resonance measurements, 1,000 resonance units of BclA-1-island-6HIS was covalently coupled to a Biacore CM3 chip using amine chemistry by activation of the carboxymethyl dextran chip surface with 1-ethyl-3-(3-dimethylaminopropyl)carbodiimide (EDC) and NHS. A reference channel was created by capping off one channel of the EDC/NHS activated CM3 chip with ethanolamine. Supernatants were injected over the biosensor surface in duplicate at a flow rate of 30 μl/min. Supernatant from nontransfected cells was intermittently injected during the course of the experiment for double referencing. The surface was regenerated after each cycle with a 30-s pulse of 50 mM NaOH, pH 12.5. Sensorgrams were processed by using BiaEvaluation (Biacore) and Scrubber2 software (BioLogic Software). Sensorgrams were zeroed on the y axis, and bulk refractive index changes were removed by subtracting the reference channel. VLR plasmid transfections and biosensor analysis were repeated four independent times.

1. Pancer Z, *et al.* (2004) Somatic diversification of variable lymphocyte receptors in the agnathan sea lamprey. *Nature* 430:174–180.
2. Pancer Z, *et al.* (2005) Variable lymphocyte receptors in hagfish. *Proc Natl Acad Sci USA* 102:9224–9229.
3. Rogozin IB, *et al.* (2007) Evolution and diversification of lamprey antigen receptors: evidence for involvement of an AID-APOBEC family cytosine deaminase. *Nat Immunol* 8:647–656.
4. Alder MN, *et al.* (2005) Diversity and function of adaptive immune receptors in a jawless vertebrate. *Science* 310:1970–1973.
5. Nagawa F, *et al.* (2007) Antigen-receptor genes of the agnathan lamprey are assembled by a process involving copy choice. *Nat Immunol* 8:206–213.
6. Finstad J, Good RA (1964) The evolution of the immune response. 3. Immunologic responses in the lamprey. *J Exp Med* 120:1151–1168.
7. Papermaster BW, Condie RM, Finstad J, Good RA (1964) Evolution of the immune response. I. The phylogenetic development of adaptive immunologic responsiveness in vertebrates. *J Exp Med* 119:105–130.
8. Marchalonis JJ, Edelman GM (1968) Phylogenetic origins of antibody structure. 3. Antibodies in the primary immune response of the sea lamprey, *Petromyzon marinus. J Exp Med* 127:891–914.
9. Litman GW, *et al.* (1970) The evolution of the immune response. VIII. Structural studies of the lamprey immunoglobulin. *J Immunol* 105:1278–1285.
10. Pollara B, Litman GW, Finstad J, Howell J, Good RA (1970) The evolution of the immune response. VII. Antibody to human ''O'' cells and properties of the immunoglobulin in lamprey. *J Immunol* 105:738–745.
11. Boydston JA, Chen P, Steichen CT, Turnbough CL, Jr (2005) Orientation within the exosporium and structural stability of the collagen-like glycoprotein BclA of *Bacillus anthracis. J Bacteriol* 187:5310–5317.
12. Steichen C, Chen P, Kearney JF, Turnbough CL, Jr (2003) Identification of the immunodominant protein and other proteins of the *Bacillus anthracis* exosporium. *J Bacteriol* 185:1903–1910.
13. Rety S, *et al.* (2005) The crystal structure of the *Bacillus anthracis* spore surface protein BclA shows remarkable similarity to mammalian proteins. *J Biol Chem* 280:43073–43078.
14. Kim HM, *et al.* (2007) Structural diversity of the hagfish variable lymphocyte receptors. *J Biol Chem* 282:6726–6732.
15. Swiecki MK, Lisanby MW, Shu F, Turnbough CL, Jr, Kearney JF (2006) Monoclonal antibodies for *Bacillus anthracis* spore detection and functional analyses of spore germination and outgrowth. *J Immunol* 176:6076–6084.
16. Roux KH (1996) Negative-stain immunoelectron-microscopic analysis of small macromolecules of immunologic significance. *Methods* 10:247–256.

IMMUNOLOGY